Optimum Design of a High-Power, High-Frequency Transformer

R. Petkov

Abstract—**A procedure for optimum design of a high-power, high-frequency transformer is presented. The procedure is based on both electrical and thermal processes in the transformer and identifies a) the VA-rating of ferrite cores in relation to the operating frequency, b) the optimum flux density in the core, and c) the optimum current densities of the windings providing maximum transformer efficiency. Since the transformer is the major contributor to the volume and weight of the power supply, the results of transformer analysis can be used for entire power supply optimization as well. Two high-power, high-frequency transformers are optimally designed, built, and tested. Practical results show good agreement with the theory.**

I. Introduction

MAGNETIC component technology has received considerable attention in recent years since it is widely recognized that the ability to manufacture small and efficient magnetic components is the key to achieving high power density. It is a well-known fact that the high-frequency transformer is the major contributor in the size of any SMPS since it determines about 25% of the overall volume and more than 30% of the overall weight. Fundamental issues in the design of any high-power, high-frequency transformer are to minimize the loss and the volume.

This paper explores the optimum design of a high-power and high-frequency transformer, which means 1) selection of the smallest standard core shape relevant to the throughput power, frequency, and transformer operating temperature, 2) calculation of the optimum flux density providing minimum transformer loss, and 3) calculation of the optimum wire diameters of the windings. In order to compile such a complex optimization procedure, investigations were carried out in the following areas:

1) core loss determination,
2) copper loss determination,
3) thermal modeling, and
4) optimization.

II. Core Loss

Core Loss Approximation

The total core loss at flux densities below saturation is a sum of three loss mechanisms [6], [24]: hysteresis, residual, and eddy current. The idea of core loss determination employed in this paper is to approximate the data sheet curves with an analytical expression using the curve fitting method [16].

Manuscript received January 10, 1995; revised May 25, 1995.
The author is with Swichtec Power Systems, Christchurch, New Zealand.
Publisher Item Identifier S 0885-8993(96)00593-5.

There are several curve fitting fit formulae used for the approximation of core loss [4], [6], [10], [12], [15], [17]–[19], and [25] originating either from the physical or geometrical interpretation of data sheet curves. The main criterion for the fit formula choice should be the approximation accuracy. In terms of that, the geometrical interpretation is more preferable, since the physical model, usually based on several simplifications, is not accurate enough. The best combination between the accuracy and simplicity seems to have the expression used in [6], [12], [15], [17], [25]

$$p_C = K1 \cdot f^{K2} \cdot B^{K3} \tag{1}$$

where

p_C [kW/m^3]	—core power loss density
f [Hz]	—frequency
B [T]	—flux density
$K1$, $K2$, and $K3$	—curve fitting formula constants.

The values of $K1$, $K2$, and $K3$ for the FERROXCUBE ferrite grades at core temperature 100°C, which provide an approximation accuracy about 20%, can be found in [17]. For the case of 3C80 grade, these values are $K1 = 16.7$, $K2 = 1.3$, $K3 = 2.5$.

III. Copper Loss

By definition, the power loss P_w in a conductor carrying ac current with a value I_{RMS} is

$$P_w = K_r \frac{\rho \cdot 1}{\mathrm{Ac}} I_{\mathrm{RMS}}^2 \tag{2}$$

where $K_r = \frac{R_{\mathrm{ac}}}{R_{\mathrm{dc}}}$ is called an ac-resistance coefficient.

Quite a few papers have been published on this subject, starting with the basic work written by Dowell [5]. Many of the following papers, [2], [7], [9], [14], [20]–[23], are to some extent related to Dowell's physical interpretation, although they have extended the analysis and made it more accurate for some particular applications. Dowell's results are in a closed form, hence very convenient to use and easily extendible on different current waveforms and winding structures. Finally, Dowell's analysis is more accurate for the case of high-power (more than 1 kVA) transformers, which have 1) quite a low magnetizing current, 2) almost complete enclosure of the winding window, and 3) ungapped core. The error introduced by replacing round conductors with square section conductors is relatively small if the normalized (to skin depth) wire diameter is smaller than 0.25, as suggested

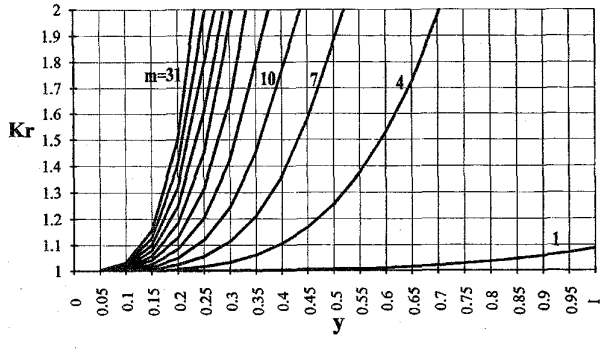

Fig. 1. Ac/dc resistance ratio of an m-layer winding.

below. This, in turn, means that the analysis is also relatively accurate for foil windings, since the latter can be represented as a number of square sections connected in parallel [7]. Therefore, the Dowell [5] interpretation of the winding ac-resistance coefficient is used in this optimization procedure, and hence the ac/dc resistance ratio K_r of the winding is

$$K_r = \frac{R_{\text{ac}}}{R_{\text{dc}}} = 0.5y[M(y) + (2m-1)^2 \cdot D(y)] \tag{3}$$

where

$$y = hc/\delta \tag{4}$$

is the normalized conductor thickness

1) for a foil conductor: hc—conductor thickness, δ—skin depth at 100°C
2) for a round conductor: $hc = 0.886$ d, (d—wire diameter)

$$\delta = \frac{0.071}{\sqrt{f}} \quad (f\text{—frequency}) \tag{5}$$

m—number of layers

$$M(y) = \frac{\sinh(y) + \sin(y)}{\cosh(y) - \cos(y)} \tag{6}$$

$$D(y) = \frac{\sinh(y) + \sin(y)}{\cosh(y) - \cos(y)}. \tag{7}$$

The relationship $K_r(m, y)$ calculated from (3) is presented graphically in Fig. 1.

One can conclude from the graphs that K_r depends very strongly on both the number of layers m and the normalized conductor thickness y. It follows that at high frequencies, associated with a small skin depth, the conductor thickness should be kept as small as possible. To achieve this practically, hence to reduce the winding loss, a "litz" wire or copper foil should be always used in the high-frequency power transformers.

An acceptable value of the normalized conductor thickness is $y < 0.25$ (Fig. 1) that results in an approximately 60% increase of the windings ac resistance, even for a large number of layers ($m = 22$). Such a small value of the normalized thickness also provides very good accuracy of Dowell's analysis [8] and determines the most suitable strand diameters of the "litz" wire used.

IV. Thermal Modeling

A. Thermal Resistances of the Transformer

1) Resistance of the Components Transferring Heat by Convection:

a) "windings ambient" thermal resistance

$$R_{\text{wa}} = \frac{1}{\lambda_w \cdot A_w} \tag{8}$$

where

λ_w —windings heat transfer coefficient
A_w —the area of the open surface of the windings

b) "core ambient" thermal resistance

- vertical surface

$$R_{\text{cv}} = \frac{1}{\lambda_{\text{cv}} \cdot A_{\text{cv}}} \tag{9}$$

where

λ_{cv} —core (vertical surface) heat transfer coefficient
A_{cv} —total area of the vertically oriented open surface of the core

- horizontal surface

$$R_{\text{ch}} = \frac{1}{\lambda_{\text{ch}} \cdot A_{\text{ch}}} \tag{10}$$

λ_{ch} —core (horizontal surface) heat transfer coefficient
A_{ch} —total area of the horizontally oriented open surface of the core

- total "core ambient" thermal resistance

$$R_{\text{ca}} = \frac{R_{\text{cv}} \cdot R_{\text{ch}}}{R_{\text{cv}} + R_{\text{ch}}}. \tag{11}$$

2) Resistance of the Components Transferring Heat by Conduction:

a) coil former thermal resistance

$$R_f = \frac{\ln \frac{r_F + \Delta_f}{r_F}}{2\pi \cdot \rho_{\Theta_f} \cdot h} \tag{12}$$

where

Δ_f —coil former thickness
ρ_{Θ_f} —coil former thermal conductivity
h —coil former height
r_F —outer radius of the coil former

b) windings thermal resistances

- primary

$$R_{w1} = \frac{\ln\left(\frac{r_1}{r_F}\right)}{2\pi \cdot \rho_{\Theta_w} \cdot h_w} \tag{13}$$

- secondary

$$R_{w2} = \frac{\ln\left(\frac{r_F + c}{r_1}\right)}{2\pi \cdot \rho_{\Theta_w} \cdot h_w} \tag{14}$$

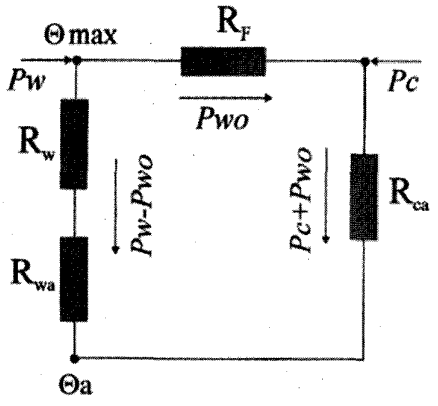

Fig. 2. Transformer thermal circuit when the hottest spot is on the windings.

- total thermal resistance of the windings

$$R_w = \frac{1}{2\pi \cdot \rho_{\Theta_w} \cdot h_w}\left[\ln\left(\frac{r_1}{r_f}\right) + \ln\left(\frac{r_F + c}{r_1}\right)\right] \tag{15}$$

where

$\rho\Theta_w$	—thermal conductivity of the windings
h_w	—height of the primary winding
r_1	—outer radius of the primary (inner radius of the secondary)
c	—coil former width.

All listed radii are shown in Fig. 4, which presents the central section of half a transformer. Thermal conductivities and heat transfer coefficients can either be taken from the literature [1], [3] or, better, measured experimentally.

B. Thermal Model of the Transformer

The equivalent thermal circuit of the transformer when the hottest spot is on the windings (the most common case) is shown in Fig. 2. In the circuit, $R_w, R_{\rm wa}, R_F, R_{\rm ca}$ are the thermal resistances, defined in Section IV-A of the windings, windings ambient, coil former, and core ambient, respectively; $\Theta_{\max}, \Theta_a$ are the temperatures of the hottest transformer spot (the windings), and the ambient temperature; P_w is winding power dissipation vector concentrated on the hottest spot $\Theta_{\max}$; and P_c is core power dissipation vector concentrated on the core surface.

The core thermal resistance, which expresses heat transfer through the core by conduction, is short-circuited in this thermal circuit due to comparatively high thermal conductivity of the ferrite material. Hence, a uniform temperature distribution inside the core is assumed, which is in line with the practical experience.

To improve the thermal model, the heat transfer inside the windings is separately studied.

Applying both Kirchhoff's and Ohm's laws to the above circuit, the following equations can be written:

$$\Theta_{\max} - \Theta_a = (P_w - P_{w0})(R_w + R_{\rm wa}) \tag{16}$$

$$(P_w - P_{w0})(R_w + R_{\rm wa}) - (P_c + P_{w0})R_{\rm ca} - P_{w0}R_F = 0. \tag{17}$$

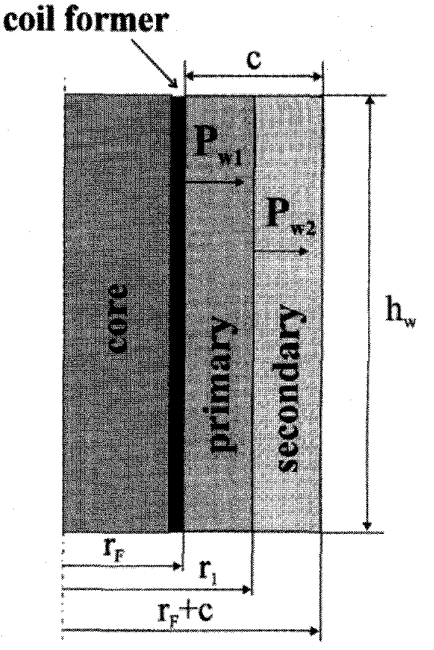

Fig. 3. Central section of the transformer half.

Solving (16) and (17) for P_{w0}

$$P_{w0} = P_w \frac{R_w + R_{\rm wa} - \frac{P_c}{P_w}R_{\rm ca}}{R_w + R_{\rm wa} + R_{\rm ca} + R_F}. \tag{18}$$

The last expression links the heat flow P_{w0} through the coil former with the power dissipation and the thermal resistances of the transformer. The value of P_{w0} should be positive for circuit validity, otherwise another thermal model must be used, i.e., (18)

$$\frac{P_c}{P_w} \le \frac{R_w + R_{\rm wa}}{R_{\rm ca}}. \tag{19}$$

Substitution of (18) into (16) yields

$$\theta_{\max} - \Theta_a = \Delta\Theta = P_w \frac{(R_w + R_{\rm wa})(R_{\rm ca} + R_F)}{R_w + R_{\rm wa} + R_{\rm ca} + R_F} \times \left(1 + \frac{R_{\rm ca}}{R_{\rm ca} + R_F}\frac{P_c}{P_w}\right). \tag{20}$$

Equation (20) shows the relationship between the temperature rise $\Delta\Theta$ of the transformer and power dissipation in its components. From this equation, one can determine P_c and then after long but straightforward mathematical manipulations one can arrive to the transformer thermal resistance

$$R_{\rm th} = \frac{\Delta\Theta}{P_w + P_c} = \frac{(R_w + R_{\rm wa})\left(R_{\rm ca} + R_F + \frac{P_c}{P_w}R_{\rm ca}\right)}{(R_w + R_{\rm wa} + R_F + R_{\rm ca})\left(1 + \frac{P_c}{P_w}\right)}. \tag{21}$$

As can be seen, transformer thermal resistance is not only a function of the component thermal resistances but of the power dissipation ratio P_c/P_w as well. The latter, as proved in Section VII of the paper, depends on the ferrite material

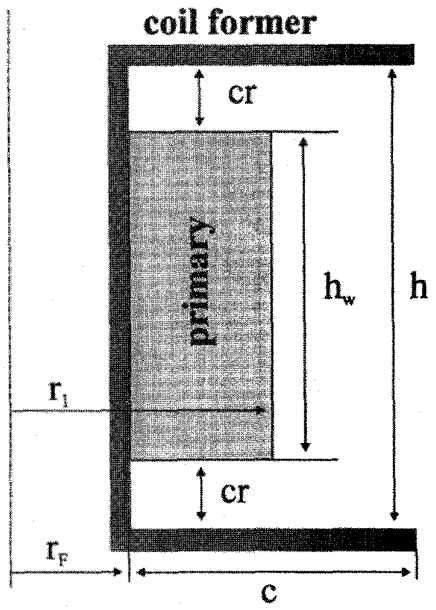

Fig. 4. Central section of the coil former and the primary halves.

and, hence, varies. Furthermore, the optimum value P_c/P_w tends to 0.8, for the majority of high power ferrite core shapes (see Section VII), not to unity as usually assumed by most of the authors.

Derived formulae exhibit clearly the nature of transformer thermal resistance formation which has not been clear from previous articles.

Finally, and most important, the thermal resistance formula is the necessary base for optimum design of the transformer since they link its thermal performance with the electrical parameters P_c and P_w.

C. Thermal Model of the Windings

A central section of a transformer half is shown in Fig. 3.

The following assumptions were made when drawing this picture:

1) The transformer has just two windings—primary and secondary. This assumption is very often valid for the high-power transformers. To use thermal modeling results for transformers with several secondaries, they must be relegated to one equivalent secondary winding carrying the total power.
2) The coil former is fully utilized; hence, the outer radius of the secondary is $r_F + c$ (Fig. 4). This is always valid when the core is properly selected.
3) Power dissipation due to copper loss is concentrated mainly on the inner radius of the winding. This assumption was based on Ferreira's [7] finite element analysis of copper loss distribution in a winding example. In fact, this is the worst case of power distribution; hence, any inaccuracy should lead practically to a slightly lower temperature.
4) The winding has a cylindrical shape. This is valid for all core types with a round leg (EC, ETD, RM, PM, P, EP, toroid shapes, some of U shapes). If the winding shape is not cylindrical, it must be replaced by an equivalent cylindrical shape having an equal a) height and b) areas of the inner and outer winding surfaces.

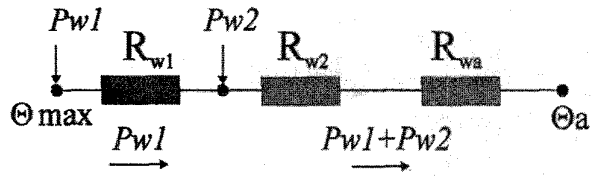

Fig. 5. Equivalent thermal circuit of the windings.

Fig. 4 shows a central section of the coil former and the primary halves and identifies the relationship between the dimensions of the coil former and the winding.

In Fig. 4, $h_w = h - 2$ cr is the winding height, and cr is the creepage required (usually 3–4 mm). The creepage may increase to 6–8 mm for high voltage transformers.

Now, one has all the information to compile the equivalent thermal circuit of the windings, as shown in Fig. 5.

In Fig. 5, P_{w1} and P_{w2} are the power loss in the primary and the secondary, R_{w1} and R_{w2} are conduction thermal resistances of the primary and the secondary, R_{wa} is the convection "windings ambient" thermal resistance, and $\Theta_{\max}$ and Θ_a are the maximum winding temperature and the ambient temperature.

Employing Kirchhoff's and Ohm's laws in the above thermal circuit yields

$$\Delta\Theta = \Theta_{\max} - \Theta_a = P_{w1} \cdot R_{w1} + (P_{w1} + P_{w2})(R_{w2} + R_{\mathrm{wa}}). \tag{22}$$

The thermal resistances in (22) can be calculated from (13), (14), and (10) accounting for the windings dimensions. Let us assign

$$x = \frac{r_1}{r_F}, \qquad K_1 = 1 + \frac{c}{r_F}, \qquad 1 \le x \le K_1. \tag{23}$$

Substitution of (23) into (13) and (14) results in

$$R_{w1} = \frac{\ln x}{2 \cdot \pi \cdot \rho_{\Theta_w} \cdot h_w} \tag{24}$$

$$R_{w2} = \frac{\ln\left(\frac{K_1}{x}\right)}{2 \cdot \pi \cdot \rho_{\Theta_w} \cdot \cdot h_w}. \tag{25}$$

The value of x obviously depends on the core type; however, it practically varies between 1.6 and 2.1. An evaluation of R_{w1} (24), R_{w2} (25), and R_{wa} (10), for several ferrite core types, shows that conduction resistances R_{w1}, R_{w2}, are much smaller than R_{wa}. This phenomenon is based on a) high thermal conductivity of the winding materials (reducing R_{w1} and R_{w2}) and b) relatively small cooling area of the windings (increasing R_{wa}). This conclusion greatly simplifies thermal circuit in Fig. 5, since R_{w1} and R_{w2} can be short-circuited. The new thermal equilibrium condition can now be obtained from (22) by equating R_{w1} and R_{w2} to zero

$$\Delta\Theta = \Theta_{\max} - \Theta_a (P_{w1} + P_{w2}) R_{\mathrm{wa}}. \tag{26}$$

From Fig. 3, it can be concluded that the electrical resistances of the windings (and their power loss) are dependent on the outer radius r_1 of the primary or on x (23). For example, a lower value of x increases the electrical resistance (and associated loss) of the primary because of the lower winding cross sectional area, but conversely decreases the electrical resistance (and associated loss) of the secondary. This correlation implies the existence of an optimum x value ensuring minimum overall loss in the windings and hence a minimum temperature difference (26). Thus, the idea of the winding thermal analysis is to find out the optimum value of x ensuring minimum temperature difference $\Delta\Theta = \Theta_{\max} - \Theta_a$.

To perform this task, the power loss values P_{w1}, P_{w2} should be defined as functions of x.

Using (6)

$$P_{w1} = I_1^2 \cdot K_{r1} \frac{\rho \cdot l_{1a} \cdot N_1}{A_{\mathrm{Cu1}}}$$
$$P_{w2} = I_2^2 \cdot K_{r2} \frac{\rho \cdot l_{2a} \cdot N_2}{A_{\mathrm{Cu2}}} \tag{27}$$

where

I_1, I_2 —RMS values of the primary and secondary currents
K_{r1}, K_{r2} —ac-resistance coefficients of the primary and secondary windings
ρ —copper conductivity
l_{1a}, l_{2a} —average lengths of the primary and secondary turns
N_1, N_2 —numbers of the primary and secondary turns
$A_{\mathrm{Cu1}}, A_{\mathrm{Cu2}}$ —pure copper cross-sectional areas of the primary and secondary wires.

Assuming for simplicity $K_{r1} = K_{r2} = K_r$, the total winding loss becomes

$$P_w = P_{w1} + P_{w2} = K_r \cdot \rho \left(I_1^2 \frac{l_{1a} N_1}{A_{\mathrm{Cu1}}} + I_2^2 \frac{l_{2a} N_2}{A_{\mathrm{Cu2}}} \right). \tag{28}$$

Taking into account the geometric definition for the average length and including (23) leads to

$$l_{1a} = 2\pi r_{1a} = 2\pi \frac{r_1 + r_F}{2} = \pi r_F (x+1) \tag{29}$$
$$l_{2a} = 2\pi r_{2a} = 2\pi \frac{r_1 + r_F + c}{2} = \pi r_F (x + K_1). \tag{30}$$

Now let us consider the primary winding in Fig. 4, as formed by N_1 turns of wire with a diameter d_1 and let us also suppose that they are equally distributed in m_1 layers. Similarly, let us assume that the secondary winding is formed by N_2 turns of wire with a diameter d_2 distributed in m_2 layers. Then, the number of turns N_{11} and N_{21} in a single layer correspondingly of the primary and of the secondary is

$$N_{11} = \frac{h_w \cdot K_{\mathrm{axial}}}{d_1}, \qquad N_{21} = \frac{h_w \cdot K_{\mathrm{axial}}}{d_2} \tag{31}$$

where K_{axial} is a space utilization factor of the wire in an axial direction, due to the incomplete compacting of the wire in the axial direction of the winding. It depends on the wire diameter and varies between 0.88 and 0.96 for wire diameters between 0.1 and 3 mm.

Then, the number of primary and secondary layers from Fig. 3 is

$$m_1 = \frac{(r_1 - r_F) \cdot K_{\mathrm{radial}} \cdot K_{\mathrm{insul}}}{d_1} = \frac{r_F (x-1) \cdot K_{\mathrm{radial}} \cdot K_{\mathrm{insul}}}{d_1} \tag{32}$$
$$m_2 = \frac{(r_2 - r_1) \cdot K_{\mathrm{radial}} \cdot K_{\mathrm{insul}}}{d_2} = \frac{r_F (K_1 - x) \cdot K_{\mathrm{radial}} \cdot K_{\mathrm{insul}}}{d_2} \tag{33}$$

where K_{insul} is a space utilization factor of the winding in a radial direction, due to the insulation between the winding layers. It depends on both the insulation thickness and the wire diameter and varies between 0.71 and 0.96 for an insulation thickness between 0.02 and 0.2 mm and a wire diameter between 0.1 and 3 mm,

K_{radial} is a space utilization factor of the wire in a radial direction, due to the incomplete compacting of the wire in the radial direction of the winding. It depends on the wire diameter and varies between 0.77 and 0.98 for wire diameters between 0.1 and 3 mm.

Taking into account that

$$N_1 = m_1 \cdot N_{11}, \qquad N_2 = m_2 \cdot N_{21} \tag{34}$$

and substituting (31), (32), and (33) into (34) yields

$$N_1 = \frac{h_w \cdot r_F \cdot (x-1) \cdot K_{\mathrm{radial}} \cdot K_{\mathrm{axial}} \cdot K_{\mathrm{insul}}}{d_1^2}$$
$$N_2 = \frac{h_w \cdot r_F \cdot (K_1 - x) \cdot K_{\mathrm{radial}} \cdot K_{\mathrm{axial}} \cdot K_{\mathrm{insul}}}{d_2^2}. \tag{35}$$

Wire diameters d_1, d_2, and their cross-sectional areas A_{w11}, A_{w21} can be easily related and elaborated using (35)

$$A_{w11} = \frac{\pi \cdot d_1^2}{4} = \frac{\pi \cdot h_w \cdot r_F \cdot (x-1) \cdot K_{\mathrm{radial}} \cdot K_{\mathrm{axial}} \cdot K_{\mathrm{insul}}}{4 N_1} \tag{36}$$
$$A_{w21} = \frac{\pi \cdot d_2^2}{4} = \frac{\pi \cdot h_w \cdot r_F \cdot (K_1 - x) \cdot K_{\mathrm{radial}} \cdot K_{\mathrm{axial}} \cdot K_{\mathrm{insul}}}{4 N_2}. \tag{37}$$

The pure copper cross-sectional areas of the wires are related to their total cross-sectional areas by the following:

$$A_{\mathrm{Cu1}} = A_{w11} \cdot K_{\mathrm{litz}} \cdot K_{\mathrm{Cu}}$$
$$A_{\mathrm{Cu2}} = A_{w21} \cdot K_{\mathrm{litz}} \cdot K_{Cu} \tag{38}$$

where K_{litz} is an area utilization factor of the "litz" wire, due to the incomplete compacting of the strands inside the "litz" bundle. It defines the ratio: total area of the strands/"litz" bundle area and its value is $\pi/4 = 0.785$. This factor is equal to 1 for the standard (not "litz") wires.

K_{Cu} is an area utilization factor of a single "litz" wire strand. It defines the ratio: pure copper cross-sectional area of the strand/total (including insulation) cross-sectional area

of the strand and depends on the strand diameter. The usual value of this factor is 0.6–0.7 for commonly used very small strand diameters.

Substitution of (37) into (38) yields

$$A_{\mathrm{cu1}} = \frac{\pi \cdot h_w \cdot r_F \cdot (x-1) \cdot K_{\mathrm{litz}} \cdot K_{\mathrm{Cu}} \cdot K_{\mathrm{radial}} \cdot K_{\mathrm{axial}} \cdot K_{\mathrm{insul}}}{4N_1} = \frac{\pi \cdot h_w \cdot r_F \cdot (x-1) \cdot K_w}{4N_1} \tag{39}$$

$$A_{\mathrm{Cu2}} = \frac{\pi \cdot h_w \cdot r_F \cdot (K_1 - x) \cdot K_{\mathrm{litz}} \cdot K_{\mathrm{Cu}} \cdot K_{\mathrm{radial}} \cdot K_{\mathrm{axial}} \cdot K_{\mathrm{insul}}}{4N_2} = \frac{\pi \cdot h_w \cdot r_F \cdot (K_1 - x) \cdot K_w}{4N_2} \tag{40}$$

where

$$K_w = K_{\mathrm{Cu}} \cdot K_{\mathrm{litz}} \cdot K_{\mathrm{radial}} \cdot K_{\mathrm{axial}} \cdot K_{\mathrm{insul}}. \tag{41}$$

K_w is an area utilization factor of the windings. This is a complex utilization factor involving all the cited utilization factors and describing the ratio: pure copper cross-sectional area of the windings/total cross-sectional area of the windings.

Now we have all the terms to define the winding power loss. Thus, accounting for $K_{r1} = K_{r2} = K_r$ and substituting (39), (29), (30), and (40) into (27) gives

$$P_{w1} = 4I_1^2 \cdot N_1^2 \cdot K_r \cdot \rho \frac{1+x}{h_w \cdot K_w (x-1)} \tag{42}$$

$$P_{w2} = 4I_2^2 \cdot N_2^2 \cdot K_r \cdot \rho \frac{K_1 + x}{h_w \cdot K_w (K_1 - x)}. \tag{43}$$

Equations (42) and (43) exhibit clearly the relationship between the winding loss and x.

Ampere-turn balance of the transformer states

$$I_1 \cdot N_1 = I_2 \cdot N_2. \tag{44}$$

Substituting it into (28) and rearranging yields

$$P_w = P_{w1} + P_{w2} = \frac{8I_1^2 \cdot N_1^2 \cdot K_r \cdot \rho}{h_w \cdot K_w} \left[\frac{x(K_1 - 1)}{(x-1)(K_1 - x)} \right]. \tag{45}$$

After substitution of (45) into (26), the latter takes the form

$$\Delta\Theta = \frac{8I_1^2 \cdot N_1^2 \cdot K_r \cdot \rho \cdot R_{\mathrm{wa}}}{h_w \cdot K_w} \left[\frac{x(K_1 - 1)}{(x-1)(K_1 - x)} \right]. \tag{46}$$

Analyzing (46) one can notice that $\Delta\Theta$ tends to infinity in the boundary cases $x = 1$ and $x = K_1$. Obviously, the temperature rise has a minimum value for some $x = x_{\mathrm{opt}}$ within the above range. A standard technique for determining the minimum value of the function was used to derive x_{opt}

$$\frac{d(\Delta\Theta)}{dx} = 0 \quad \text{which results in } x_{\mathrm{opt}} = \sqrt{K_1}. \tag{47}$$

Substitution of (47) into (46) and (45) gives the minimum temperature rise value and the minimum power loss value, respectively

$$\Delta\Theta_{\min} = \frac{8I_1^2 \cdot N_1^2 \cdot K_r \cdot \rho \cdot R_{\mathrm{wa}}}{h_w \cdot K_w} \left[\frac{\sqrt{K_1} + 1}{\sqrt{K_1} - 1} \right] \tag{48}$$

$$P_{w_{\min}} = \frac{8I_1^2 \cdot N_1^2 \cdot K_r \cdot \rho}{h_w \cdot K_w} \left[\frac{\sqrt{K_1} + 1}{\sqrt{K_1} - 1} \right]. \tag{49}$$

It is important to know what the optimum power distribution between the primary and the secondary windings is. To define this, the optimum x value (47) has to be substituted into (42) and (43)

$$\frac{P_{w1_{\mathrm{opt}}}}{P_{w2_{\mathrm{opt}}}} = 1 \quad \text{or} \quad P_{w_{\mathrm{opt}}} = 2P_{w1}. \tag{50}$$

Thus, an important result was deduced from the winding thermal analysis that the total loss in the windings is minimum when it is equally distributed between the primary and the secondary.

Using derived expressions and the correlation between the electrical and the magnetic parameters of the transformer, one can derive expressions for the optimum winding loss and optimum current densities as functions of the output power.

V. Optimum Value of the Winding Loss

As derived before (47), the optimum value of the outer diameter of the primary winding is

$$r_{1\mathrm{opt}} = r_F \cdot x_{\mathrm{opt}} = r_F \sqrt{1 + \frac{c}{r_F}}. \tag{51}$$

The following equations are valid for the transformer:

$$I_1 = \frac{P_0}{V_1} \tag{52}$$

$$N_1 = \frac{V_1}{4 \cdot K_{\mathrm{sh}} \cdot B \cdot A_e \cdot f} \tag{53}$$

where

- P_0 —VA rating of the transformer
- V_1 —RMS value of the primary voltage
- K_{sh} —shape coefficient of the primary voltage. This coefficient is equal to unity for the case of a rectangular shape of the primary voltage, and to 1.11 for the case of a sinusoidal shape
- B —magnitude of the operating flux density in the core
- A_e —cross-sectional area of the core
- f —operating frequency.

Multiplying (52) and (53)

$$I_1 \cdot N_1 = \frac{P_0}{4 \cdot K_{\mathrm{sh}} \cdot B \cdot A_e \cdot f}. \tag{54}$$

Substituting this term and (51) into (49) gives the following equation for the winding loss

$$P_w = K_{t1} \frac{P_0^2}{B^2 \cdot f^2} \tag{55}$$

where

$$K_{t1} = \frac{K_r \cdot \rho}{2 \cdot K_{\mathrm{sh}}^2 \cdot A_e^2 \cdot h_w \cdot K_w} \left[\frac{\sqrt{1 + \frac{c}{r_F}} + 1}{\sqrt{1 + \frac{c}{r_F}} - 1} \right]. \tag{56}$$

VI. Optimum Current Density of the Windings

Current densities of the windings are given by

$$J_1 = \frac{I_1}{A_{\mathrm{Cu1}}} \quad \text{and} \quad J_2 = \frac{I_2}{A_{\mathrm{Cu2}}} \tag{57}$$

where $A_{\mathrm{Cu1}}, A_{\mathrm{Cu2}}$ are pure copper cross-sectional areas of the primary and secondary wires.

The following emerges from (57)

$$\frac{J_1}{J_2} = \frac{A_{\mathrm{Cu1}} \cdot I_1}{A_{\mathrm{Cu2}} \cdot I_2}. \tag{58}$$

Substituting (39) and (40) in (58) and accounting for (44) yields

$$\frac{J_1}{J_2} = \frac{K_1 + x_{\mathrm{opt}}}{x_{\mathrm{opt}} + 1}. \tag{59}$$

Finally, substituting the optimum value of x (47) into (59) gives

$$\frac{J_{1\mathrm{opt}}}{J_{2\mathrm{opt}}} = \sqrt{K_1} = \sqrt{1 + \frac{c}{r_F}}. \tag{60}$$

The next task is to define the particular values of the current densities, which can be done by a substitution of (39) into (58)

$$\begin{aligned} J_1 &= \frac{4 \cdot I_1 \cdot N_1}{\pi \cdot h_w \cdot r_F \cdot K_w \cdot (x_{\mathrm{opt}} - 1)} \\ &= \frac{4 \cdot I_1 \cdot N_1}{\pi \cdot h_w \cdot r_F \cdot K_w \cdot \left(\sqrt{1 + \frac{c}{r_F}} - 1\right)}. \end{aligned} \tag{61}$$

The term $I_1 \cdot N_1$ has been already derived in (54), thus (61) becomes

$$J_{1\mathrm{opt}} = \frac{P_0}{\pi \cdot K_{\mathrm{sh}} \cdot B \cdot f \cdot A_e \cdot h_w \cdot r_F \cdot K_w \cdot \left(\sqrt{1 + \frac{c}{r_F}} - 1\right)}. \tag{62}$$

The current density of the secondary winding can be obtained from (60)

$$J_{2\mathrm{opt}} = \frac{J_{1\mathrm{opt}}}{\sqrt{K_1}} = \frac{J_{1\mathrm{opt}}}{\sqrt{1 + \frac{c}{r_F}}}. \tag{63}$$

VII. Transformer Optimization

The basis for transformer optimization can be derived from expressions (1) and (56) linking power loss in the windings P_w and in the core P_c with the values of the flux density B and frequency f. The total P_t transformer loss is

$$\begin{aligned} P_t &= P_c + P_w \\ &= p_c \cdot V_e + P_w \\ &= K1 \cdot V_e \cdot f^{K2} \cdot B^{K3} + K_{t1} \frac{P_0^2}{B^2 \cdot f^2} \end{aligned} \tag{64}$$

where V_e is a core volume.

From the mathematical point of view, the above expression has obviously a minimum value in the $B \cdot f$ domain, since the first term is directly and the second term inversely proportional to the product $B \cdot f$. In other words, there is an optimum flux density value $B_{\mathrm{opt_{eff}}}$, for a given frequency f, providing minimum power loss and hence maximum transformer efficiency.

The same conclusion was drawn in [3], [11], and [13], but all cited authors have not explored thoroughly the derivation of the constants in (64).

The optimization task here is to derive the optimum value B_{opt} of the flux density for a given frequency and to determine power capabilities of several ferrite cores most suitable for high power applications.

Substitution of (21) into (64) and rearranging for P_0 gives

$$P_0^2 = \frac{\Delta\Theta}{R_{\mathrm{th}} \cdot K_{t1}} B^2 \cdot f^2 - K1 \cdot V_e \cdot f^{K2} \cdot B^{K3}. \tag{65}$$

The above expression shows the relationship between the transferred power (VA rating) of the core P_0 and the product $B \cdot f$; hence, it can be used to determine core VA rating for given frequency and flux density. It also has a maximum value P_0 max, for a given frequency, which can be calculated from

$$\frac{dP_0^2}{dB}(f = \mathrm{const}) = 0 \tag{66}$$

which results in

$$B_{\mathrm{opt}_{P_0}} = \left(\frac{2\Delta\Theta}{K1 \cdot V_e \cdot (K3 + 2) \cdot R_{\mathrm{th}} \cdot f^{K2}}\right)^{\frac{1}{K3}}. \tag{67}$$

Substitution of (67) into (65) yields the value of the core VA rating (maximum VA product that can be transferred by the core)

$$\begin{aligned} &P_0 \max \\ &= \left[\frac{\Delta\Theta}{R_{\mathrm{th}} \cdot K_{t1}} \left(\frac{2\Delta\Theta}{K1 \cdot V_e \cdot (K3 + 2) \cdot R_{\mathrm{th}}}\right)^{\frac{2}{K3}} \cdot f^{\frac{2(K3-K2)}{K3}} - \frac{K1 \cdot V_e}{K_{t1}} \right. \\ &\left. \times \left(\frac{2\Delta\Theta}{K1 \cdot V_e \cdot (K3 + 2) \cdot R_{\mathrm{th}}}\right)^{\frac{K3+2}{K3}} \cdot f^{\frac{2(K3-K2)}{K3}}\right]^{0.5}. \end{aligned} \tag{68}$$

As (68) shows, the core VA rating is a quite complicated function of the frequency, temperature rise, ferrite material parameters, and geometry of both the core and the windings.

It should be emphasized here, that derived optimum value $B_{\mathrm{opt}_{P_0}}$ provides maximum core VA rating, however not maximum efficiency (minimum transformer power loss). As mentioned in the beginning of this section, there is another optimum value $B_{\mathrm{opt_{eff}}}$, ensuring minimum total loss and maximum transformer efficiency.

This value can be defined from (64) by equating to zero its first derivative

$$\frac{dP_t}{dB}(f = \mathrm{const}) = 0 \tag{69}$$

which results in

$$B_{\mathrm{opt}_{P_0}} = \left(\frac{2 \cdot K_{t1} \cdot P_0^2}{K1 \cdot V_e \cdot K3 \cdot f^{K2+2}}\right)^{\frac{1}{K3+2}}. \tag{70}$$

Minimum transformer loss value can be determined by a substitution of (70) into (64)

$$P_{t\min} = K1 \cdot V_e \cdot f^{\frac{2(K2-K3)}{K3+2}} \left(\frac{2K_{t1} \cdot P_0^2}{K1 \cdot K3 \cdot V_e} \right)^{\frac{K3}{K3+2}} + K_{t1} \cdot P_0^2 \left(\frac{2K_{t1} \cdot P_0^2}{K1 \cdot K3 \cdot V_e} \right)^{\frac{-2}{K3+2}} \cdot f^{\frac{2(K2-K3)}{K3+2}}. \quad (71)$$

The question now is Which one of the derived optimum values $B_{\mathrm{opt}_{P_0}}$ and $B_{\mathrm{opt}_{\mathrm{eff}}}$ should be used in the transformer design? Probably, the best result can be achieved by using both of them. Thus, $B_{\mathrm{opt}_{P_0}}$ should be used in the very beginning of the design procedure for a selection of the core type. This can be done using VA-rating graphs for several, most suitable cores made of various ferrite grades. Then, $B_{\mathrm{opt}_{\mathrm{eff}}}$ should be used to improve transformer efficiency if the margin "core VA rating"—"transformer VA rating given" is substantial, for example, more than 20–30% of the core VA rating. This happens quite often at high power levels (more than 3 kVA) because of the very limited number of core types available.

The optimum distribution of the core and winding loss for the case of maximum transformer efficiency can be deduced from division of (71) since its first term represents core loss and the second-winding loss

$$\left(\frac{P_c}{P_w} \right)_{\mathrm{opt}} = \frac{2}{K3}. \quad (72)$$

Applying the same technique for (68), expressing the core VA rating, one can find out that the loss distribution is exactly as in (72). Hence, an important conclusion arises: The optimum distribution between core and winding loss is only a function of ferrite material properties and can be calculated from (72).

Referring to [17], it can be seen that the value of $K3$ varies within the range 2.25–2.9, but for most of the ferrites it is around 2.5. It results in a optimum ratio

$$\left(\frac{P_c}{P_w} \right)_{\mathrm{opt}} \approx 0.8. \quad (73)$$

Now we have all the expressions to compile a procedure for optimum design of a high-frequency transformer.

VIII. Design Procedure of a High Frequency Transformer

The aim of the design procedure is to convert the transformer input data such as VA rating, frequency, voltage, ferrite material data, etc., into data, allowing us to assemble a real transformer, such as the type of the core, the numbers of turns of the primary and secondary windings, and the cross-sectional areas of the primary and secondary wires. In terms of that conversion, Sections IV–VII provide all the information needed.

To compile a flowchart of the transformer design procedure, one has to start from the end of the chart, i.e., from the desired final data and gradually build up a structure supporting its calculation. Fig. 6 presents a flowchart based on such an approach.

It is interesting to notice that the INPUT DATA section (Fig. 6) can be separated into several groups according to its physical nature: electrical and thermal data of the transformer, ferrite material data, coil former and core geometry data, thermal properties data and windings geometry data. Furthermore, all intermediate expressions to calculate the OUTPUT DATA (windings parameters) are separated into several CALCULATION sections and can be found from the foregoing analysis and optimization.

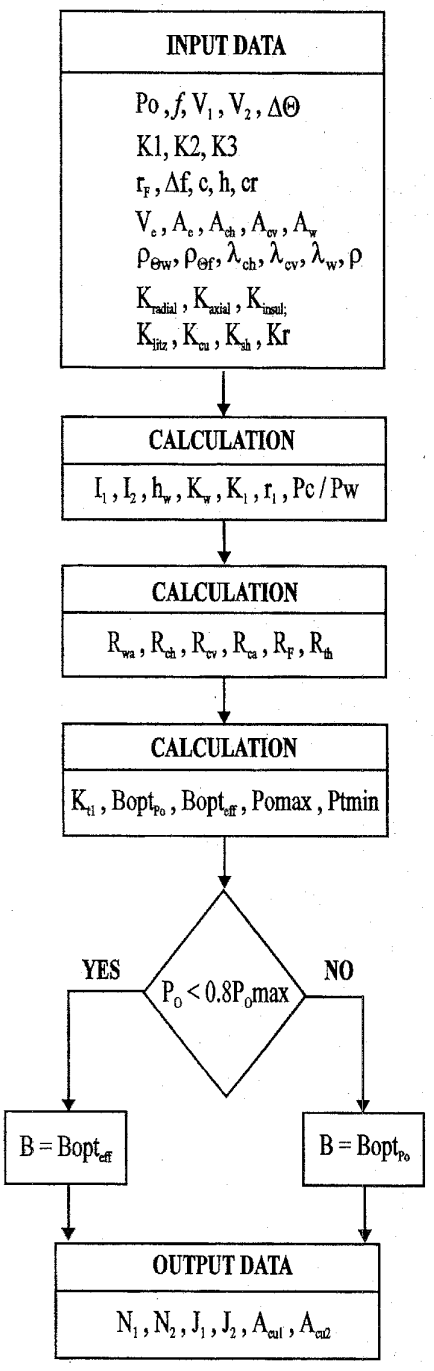

Fig. 6. Flowchart of the transformer design procedure.

As can be seen, both core geometry and core material data are given (INPUT DATA in Fig. 6), which means that the

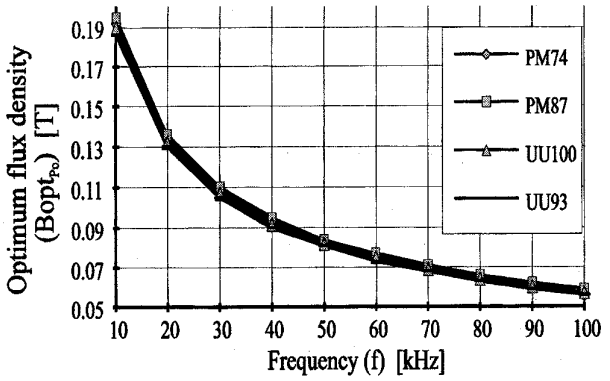

Fig. 7. Optimum flux density of high power cores (3C80).

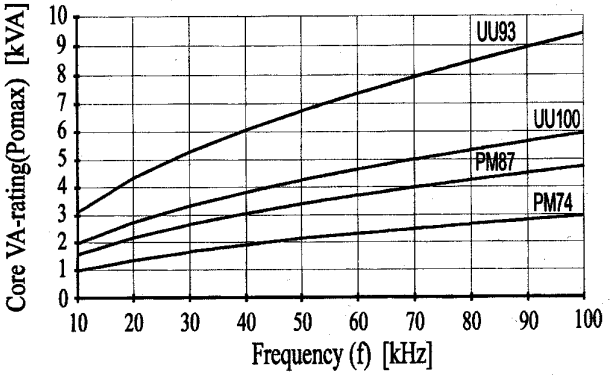

Fig. 8. VA rating of high power cores (3C80 ferrite).

type of the core has been already selected. Such a selection was based on information about the VA-rating of several cores suitable for high power conversion which was obtained by executing the flowchart partly (until $P_{0\,\max}$ calculation) for several cores at various frequencies and plotting the results (Fig. 8).

Figs. 8 and 9 show graphs of the optimum flux density and VA rating of PM 74, PM 87, UU 100, and UU 93 core types made of 3C80 ferrite grade, which were calculated using the above procedure.

As can be seen from Fig. 7, the optimum flux density is almost independent of the core. This is because the product $V_e \cdot R_{\text{th}}$ is almost constant for the core types mentioned.

The core VA-rating graphs in Fig. 8 are very useful, since they allow an optimum selection of the type of the core for a given transformer VA rating and frequency, and in terms of that, they could be used for power supply optimization as well. The number of core types and core materials in Figs. 8 and 9 can be easily increased, supplying the relevant input data of the core geometry and core material needed by the calculating procedure.

IX. Design Examples

Table I contains the specifications and the design results of two high-frequency transformers used for microwave heating SMPS. All the results were taken from the outlined procedure.

TABLE I
Design Results of High-Frequency Power Transformers

Specifications	Transformer #1	Transformer #2
VA-rating [VA]	2600	4900
Frequency [kHz]	100	40
Input voltage (rms) [V]	335	385
Output voltage (rms)[V]	5360	3970
Temperature rise [°C]	40	40
DESIGN RESULTS		
Core type	PM 74	UU 93
Ferrite grade	3C80	3C80
Number of primary turns	20	32
Number of secondary turns	320	330
Copper area of the primary wire [mm^2]	2.1	8.55
Copper area of the secondary wire[mm^2]	0.17	1.16

Using these results, the transformer prototypes were assembled and tested.

Thermal performance of the 4900 VA transformer was tested under nominal working conditions in a 2500 W magnetron power supply prototype. Two thermocouples were used: one in the center of the outermost layer of the primary winding (between primary and secondary) and the second half way up the open horizontal core surface. The ambient temperature was 25°C, and since the transformer temperature rise was predicted to be 40°C, the predicted temperature of the windings (the hottest spot) was calculated to be $25 + 40 = 65$°C. Predicted temperature of the core was calculated to be $25 + 39.1 =$

TABLE II
THERMAL PERFORMANCE OF THE 4900 VA TRANSFORMER

Temperature [°C]	Core surface	Winding
Predicted value	64.1	65
Measured value	73.7 ±1° C	75.1 ±1° C

64.1°. Table II presents temperatures measured once thermal equilibrium was reached (two hours after the prototype was switched on). It shows about 15% difference between the predicted and practical values.

X. CONCLUSION

A thermal model of a high-frequency transformer has been developed and an analytical expression for transformer thermal resistance has been derived. Based on the electrical and thermal analysis of the transformer, the following optimum values have been derived: 1) power loss distribution in the windings and windings-core, 2) primary and secondary winding thickness, 3) current density of the windings, 4) flux densities in the core providing maximum core VA rating and maximum transformer efficiency.

A procedure for optimum design of the transformer has been presented, which allows us to calculate the VA rating of various suitable cores, then to select the core and to design the whole transformer. As a first step in this design procedure, the core type has to be selected from the core VA-rating graphs, and then transformer parameters should be calculated using the optimum flux density value providing maximum transformer efficiency. The design procedure flowchart allows us to compile a computer program and to extend the design results over various core types and core materials.

Both the electromagnetic and thermal analysis of the transformer in this paper are one-dimensional; therefore, they cannot generally deliver very good accuracy. In terms of that, the main advantage of the design procedure developed is that it allows us to select the core and calculate winding parameters, i.e., it provides (with acceptable accuracy) the most necessary design information. This information can be further used for more precise (finite element or finite difference) analysis of the electromagnetic and thermal fields, associated loss, and temperatures and correction, if necessary, of the winding parameters.

Two high-power, high-frequency transformers for microwave heating SMPS have been calculated, assembled, and tested. The experimental results agreed well with the theory.

REFERENCES

[1] I. Belopolski, "Design of transformers and inductors," Energy 1973 (in Russian).

[2] B. Carsten, "High frequency conductor losses in switchmode magnetics," in *Proc. HFPC '86*, 1986, pp. 155–176.

[3] N. Conrood, "Transformer computer design aid for high frequency switching power supplies," *IEEE Trans. Power Electron.*, pp. 248–256, Oct. 1986.

[4] L. Dixon, "Design of power transformer," *UNITRODE Power Supply Design Seminar*, 1989.

[5] P. Dowell, "Effects of eddy currents in transformer windings," *IEE Proc.*, vol. 113, pp. 1387–1394, Aug. 1966.

[6] A. Estrov, "Power transformer design for 1 MHz resonant converter," in *Proc. HFPC '86*, 1986, pp. 36–54.

[7] J. Ferreira and J. Wyk, "A new method for the more accurate determination of conductor losses in power electronic converter magnetic components," in *Proc. PEVD '88*, 1988, pp. 184–187.

[8] J. Ferreira, "Analytical computation of ac resistance of round and rectangular litz wire windings," in *IEE Proc.-B*, Jan. 1992, no. 1, pp. 21–25.

[9] A. Golberg *et al.*, "Issues related to 1-10 MHz transformer design," in *Proc. PESC '87*, pp. 379–386.

[10] A. Golberg and M. Schlecht, "The relationship between size and power dissipation in a 1–10 MHz transformer," *IEEE Trans. Power Electron.*, pp. 157–167, Apr. 1992.

[11] J. Hendriks, "Optimising transformers for power conversion," in *Proc. SATECH '87*, 1987, pp. 556–567.

[12] W. Hurley and M. O'Brien., "Issues related to computer aided design of high frequency transformers," in *Proc. UPEC '91*, 1991, pp. 501–504.

[13] M. Ivancovic, "Optimum SMPS transformer design," in *Proc. PCI '86*, 1986, pp. 183–188.

[14] J. Jongsma, *High Frequency Ferrite Power Transformer and Choke Design*, Philips Tech. Pub. No. 207, Philips 1986.

[15] W. Kiefel, "Design considerations for magnetic components in switch mode power supplies," in *Proc. POWER UK '87*, 1987, pp. 1–24.

[16] *MATHCAD 4.0, User's Guide. Windows Version*, MathSoft Incorporation, 1993.

[17] S. Mulder, "Fit formulae for power loss in ferrites and their use in transformer design," in *Proc. PCIM '93*, 1993, pp. 345–359.

[18] K. Ngo *et al.*, "Design issues for the transformer in a low voltage power supply with high efficiency and high power density," *IEEE Trans. Power Electron.*, pp. 592–560, July 1992.

[19] R. Petkov and L. Hobson, "Optimum design of a high frequency transformer," in *Proc. UPEC '92*, 1992, pp. 279–282.

[20] K. Sakakibara and N. Murami, "Analysis of high frequency resistance in transformers," in *Proc. PESC '89*, 1989.

[21] J. Spreen, "Electrical terminal representation of conductor loss in transformers," *IEEE Trans. Power Electron.*, pp. 424–429, Oct. 1990.

[22] J. Vandelac and P. Ziogas, "A novel approach for minimizing high frequency transformer copper losses," *IEEE Trans. Power Electron.*, pp. 266–276, July 1988.

[23] P. Venkatraman, "Winding eddy current losses in switch mode power transformers due to rectangular wave currents," in *Proc. POWERCON 11*, 1984, pp. 1–11.

[24] E. Visser and A. Shpilman, "New power ferrite operates from 1–3 MHz," in *PCIM Europe*, Jan./Feb. 1992, pp. 24–26.

[25] W. Waanders, "Optimized ferrites and core shapes for high frequency power conversion," in *PCIM Europe*, Mar./Apr. 1993, pp. 50–51.

R. Petkov received the B.Sc. degree from the Moscow Institute of Power Engineering, Russia, and two Ph.D. degrees in electrical engineering from the Sofia Technical University, Bulgaria, and the University of Teesside, U.K., in 1974, 1983, and 1994, respectively.

He has worked as a Design Engineer at a major manufacturer of high-power, high-frequency converters in Bulgaria and as Lecturer and Associated Professor at Gabrovo Technical University (Bulgaria). In 1991 he joined the University of Teesside and in 1994 Swichtec Power Systems, New Zealand, as Leader of a research team working in the area of high-frequency power conversion. He has written about 40 publications on resonant and soft-switching power converters. His research interests are in resonant and quasi-resonant power conversion, power factor correction techniques, and high-frequency magnetics.